

UCLA

UCLA Electronic Theses and Dissertations

Title

From Traumatic Brain Injury to Tauopathy: Exploring the Mechano-Chemical Pathway

Permalink

<https://escholarship.org/uc/item/0pt6n0wb>

Author

Hosseini, Helia

Publication Date

2021

Peer reviewed|Thesis/dissertation

UNIVERSITY OF CALIFORNIA

Los Angeles

From Traumatic Brain Injury to Tauopathy: Exploring the Mechano-Chemical Pathway

A thesis submitted in partial satisfaction
of the requirements for the degree Master of Science
in Bioengineering

by

Helia Hosseini

2021

ABSTRACT OF THE THESIS

From Traumatic Brain Injury to Tauopathy: Exploring the Mechano-Chemical Pathway

by

Helia Hosseini

Master of Science in Bioengineering

University of California, Los Angeles, 2021

Professor Hossein Pirouz Kavehpour, Chair

Biomolecules in solutions subjected to extensional strain can form aggregates which may be important for our understanding of pathologies involving insoluble protein structures where mechanical forces are thought to be causative (i.e. tau fibers in chronic traumatic encephalopathy (CTE)). To examine the behavior of biomolecules in solution under mechanical strains requires applying rheological methods, often to very small sample volumes. There were two primary objectives in this investigation: 1) To probe flow-induced aggregation of proteins in microliter-sized samples and 2) To test the hypothesis that tau protein aggregates under extensional flow. Tau protein (isoform:3R 0N; 36.7 kDa) was divided into 10 microliter droplets and subjected to extensional strain in a modified tensiometer. Sixteen independent tests were performed where one test on a single droplet comprised 3 extensional events. To assess the rheological performance of the fluid/tau mixture, the diameter of the filament that formed during extension was tracked as function of time and analyzed for signs of aggregation (i.e. increased relaxation time). The results were compared to two molecules of similar and greater size (Polyethylene Oxide: PEO35, 35 kDa

and PEO100, 100 kDa). Analysis showed that the tau protein solution and PEO35 are likely to have formed aggregates, albeit at relatively high extensional strain rates (~10kHz). The investigation demonstrates an extensional rheological method capable of determining the properties of protein solutions in microliter volumes and that tau protein can aggregate when exposed to a single extensional strain with potentially significant biological implications.

The thesis of Helia Hosseini is approved.

Jeffrey D. Eldredge

Daniel T. Kamei

Hossein Pirouz Kavehpour, Committee Chair

University of California, Los Angeles

2021

DEDICATION

I would like to dedicate this work to my mother.

Without her, none of this would have been possible.

TABLE OF CONTENTS

Chapter 1: Introduction to tauopathy	1
Tau Gene and Protein	1
Tau Protein Biochemical Properties	2
Physiological Functions of Tau Protein in The Cell.....	2
Mechanistic Linkage of Traumatic Brain Injury to Tau Protein Aggregation	5
The Metabolic Crisis Cascade	6
The Neuroinflammation Cascade	9
A New Angle to Look at the Relation of Traumatic Brain Injury to Tau Protein Aggregation	19
Chapter 2: Introduction to Flow-induced Crystallization.....	21
Flow-induced Aggregation	22
Rheology of Small Samples.....	23
Tau in traumatic brain injury and localization of tau aggregation to regions of high strain	23
Chapter 3: Materials and Methods	25
Methods	27
Microextensional Rheology	28
Chapter 4: Results	32
Tau Shear Rheology.....	32
PEO Microrheology Benchmarking	32
Tau Microextensional Rheology.....	33
Analysis	34

Chapter 5: Discussion	37
Chapter 6: Conclusions and Future Work.....	40
References.....	42

LIST OF FIGURES

Figure 1: A broad approach to the mechanistic links of traumatic brain injury (TBI) to Tauopathy.

Figure 2: Microrheological test apparatus. A droplet of tau solution was placed on a hydrophobic surface and extensionally strained using a platinum rod.

Figure 3: PEO35 rheological plot and images. A) Plot of the normalized liquid bridge radius versus time for a single run. The radius versus time function was fit to the visco-elastic regime. Extensional relaxation time was $3.04e-05 \pm 7e-06$ s. B) Series: Corroborating images of liquid bridge thinning. (Blue line is fit to the viscoelastic response region of radius decay against time plot) The nozzle radius is 0.5 mm.

Figure 4: PEO100 plot and images. A) Plot of the normalized liquid bridge radius versus time for a single run. The radius versus time function was fit to the visco-elastic regime. Extensional relaxation time was $6.703e-04 \pm 6e-06$ s. B) Series: Corroborating images of liquid bridge thinning. (Blue line is fit to the viscoelastic response region of radius decay against time plot) The nozzle radius is 0.5 mm.

Figure 5: Tau rheological plot and images. A) Plot of the normalized liquid bridge radius versus time for a single run. The radius versus time function was fit to the visco-elastic regime. Extensional relaxation time was $3.6e-05 \pm 1.19e-05$ s. B) Series: Corroborating images of liquid bridge thinning. Red dashed line is fit to the viscoelastic response, and green dashed line is fit to the inertia-capillary response of radius decay against time plot). The radius of the nozzle is 0.5 mm.

Figure 6: The bar chart shows the time constants calculated from all 48 tests that were run on 16 droplets, total average extensional relaxation time is $3.6e-05 \pm 1.19e-05$. The dashed line is the theoretically calculated Zimm relaxation time.

LIST OF SYMBOLS

C^* : Overlap Concentration

M : Molar Concentration

N_A : Avogadro Number

h_0 : Root-mean-square of end-to-end distance

ϕ : Flory constant

η : Intrinsic Viscosity

$R(t)$: Radius at given time point

R_0 : Initial radius

G_E : Elastic modulus

σ : Surface tension

λ_E : Extensional relaxation time

t_c : Bridge cut-off time

t : Time

E : Elastic force

$$F = \sum_{i=1}^N 1/i^{3v}$$

v : Solvent dimensionless scaling component

M_w : Molecular weight

η_s : Solvent viscosity

R : Universal gas constant

T : Temperature

λ_{Zimm} : Zimm relaxation time

ACKNOWLEDGEMENTS

I would like to thank my adviser, Dr. H. Pirouz Kavehpour, for giving me the chance to become an undergraduate researcher, encouraging and helping me to continue on to graduate school, and having the patience and wisdom to see me through the completion of this work. In addition, I would like to thank Dr. Jeffrey Ruberti, Dr. Christopher Giza, Dr. Mayumi Prins and Dr. Aysan Rangchian for their assistance and guidance on this project. I would also like to thank Dr. Jeff Eldredge and Dr. Daniel Kamei for being on my MS thesis committee.

I would like to thank my parents for always supporting me, even if it was difficult for them and giving me a chance at an education and a better future – this is the first step, and it is all because of you.

CHAPTER 1: INTRODUCTION TO TAUOPATHY

Tau protein (Figure 1) is a microtubule binding protein involved in stabilizing the skeleton of neurons in both the CNS and PNS. Ever since discovery of its aggregated form's involvement in Alzheimer's disease pathology, tau protein has received increased attention to elucidate the mechanisms of its transformation to pathologic form. In the upcoming paragraphs, a background on the gene encoding tau protein, the protein's structure and physiological role.

TAU GENE AND PROTEIN

The tau protein gene is on the long arm of chromosome 17 (17q21) and has at least 16 exons spanning over 100kb (Tapia-Rojas *et al.*, 2019). Its regulation is primarily directed by alternative splicing. This gene is expressed in the CNS and PNS, however, the isoforms are variant and the ones in PNS are heavier (100kda) in relationship to the isoforms in the CNS (48-67kda)(Zempel *et al.*, 2017).

The isoforms in CNS are divided into two major groups of 3 and 4 repeats (difference on exon 10) on the N terminal side that correspond to the microtubule binding area. The 3R and 4R groups branch into groups of 0, 1 and 2 inserts corresponding to the C terminal repeats of tau protein (the flanking region) for binding other proteins. The difference in the number of the inserts is determined by exon 2 and 3 splicing. A protein can contain neither exon 2 nor exon 3, exon 2 and both of the mentioned (exon 3 cannot appear independently).

Therefore, as a result of this alternative splicing tau proteins of CNS are comprised of 6 isoforms (Buée *et al.*, 2000).

TAU PROTEIN BIOCHEMICAL PROPERTIES

Tau protein isoforms consist of 352-441 amino acid residues. This protein has rather distinct characteristics due to its high proportion of hydrophilic residues and many proline residues and is considered an intrinsically disordered/ Gaussian polymer- lacking a secondary structure. Tau will maintain its microtubule binding abilities even after exposure to these denaturing agents (Schweers *et al.*, 1994) like dilute acid solutions and heat. Therefore, tau is considered a 'natively denatured' protein. Tau assembles into dimers by forming cysteine di-sulfide bonds in presence of oxidizing agents, analysis of these dimers with electron micrography and X-ray crystallography shows that these structures have an antiparallel rod-like form (Goedert and Jakes, 1990).

Tau exists in the cytoplasm at a physiological range of 1 to 10 micromolar (Chirita, Necula and Kuret, 2003) (Kuret *et al.*, 2005); some lines of evidence suggest that this value is approximately 2 micromolar (Khatoon, Grundke-Iqbal and Iqbal, 1992). In comparison to other proteins tau has a concentration of 0.9 ± 0.2 ng per micrograms of protein (Khatoon, Grundke-Iqbal and Iqbal, 1992).

PHYSIOLOGICAL FUNCTIONS OF TAU PROTEIN IN THE CELL

As previously mentioned, tau takes part in various roles in the cell. For taking part in these roles this protein is required to undergo a number of post-translational modifications. In

the following paragraphs, the necessary modifications for taking part in the various roles tau has in the cell is further elaborated.

Phosphorylation, an extensively studied post translational modification, is an important determinant of tau protein localization and physiological function in axons, somatodendritic compartment, plasma membrane or nucleus nucleolar organizing regions. Staining with antibody Tau-1 (marking tau proteins that are not phosphorylated between residues 189 and 207) (Khatoon, Grundke-Iqbal and Iqbal, 1992) showed immunoreactivity in axons, while tau-1 phosphatase antibody revealed immune-reactivity in the somatodendritic compartment (Papasozomenos, 1997).

Axonal tau protein has a role in axonal processes extension and retraction and this role is mediated by phosphorylation with various kinases acting on Serine, Threonine, Proline and recently discovered Tyrosine kinases. In the process of neurite outgrowth enhancement/repression microtubule affinity regulating kinase (MARK), being a part of the adenosine monophosphate protein kinases (AMPKs) that itself is a branch of the calcium/calmodulin dependent protein kinases (CAMKs) (Timm *et al.*, 2008), is the promoter of neurite outgrowth and reduction of affinity to microtubules; while glycogen synthase kinase (GSK) is responsible for neurite retraction. Cyclin dependent kinase (cdk5) is an important regulator in neuronal positioning during development and presumably in synaptogenesis and neurotransmission. Cdk5 and GSK are a part of the PDPKs (proline dependent protein kinases) alongside many other microtubules associated protein kinases. Kinases of this family phosphorylate Ser/Thr epitopes and subsequent proline epitopes. As for GSK, the Thr-231 epitope is of significant importance (Avila *et al.*, 2004), peptidyl prolyl isomerase

converts cis tau to trans, exposing this epitope to phosphatases dephosphorylating it and enhancing tau-microtubule affinity (Tapia-Rojas *et al.*, 2019). Besides phosphorylation, other post-translational modifications can effect tau-microtubule affinity, such as methylation at lysine residues, that by neutralizing the charges of the microtubule binding domain reduces the microtubule binding ability of tau. Nitration, which is mediated by reactive nitrogen species (NO_2 and ONOO^-) at tyrosine residues decreases the strength of the tau and tubulin bond and tubulin assembly (Reynolds *et al.*, 2006).

Tau is a protein that is abundant in the cytoplasm and a significant proportion of tau has been found in the membrane in an unphosphorylated state. A study on mice showed that inhibition of casein kinase (CK1) or GSK-3 leads to decrease of tau phosphorylation and an increase in its membrane fraction. However, the localization of tau to the membrane is dependent to Fyn kinase activation (Pooler, Usardi and Hanger, 2010); where it can interact with membrane associated proteins. Fyn-tau interaction regulates the NMDA receptor signaling via binding to the NR-2B subunit involved in the post synaptic dendrite signaling (Tapia-Rojas *et al.*, 2019).

Tau also has a role in maintenance and protection DNA and RNA in the nucleus (Tapia-Rojas *et al.*, 2019). Investigation showed that there is an association between tau and pericentromeric satellite DNA; this binding is mostly in A-T base rich regions. A significant portion of tau has been found in the nucleolus; nucleolar tau reportedly localizes to the short arms at the NORs (nucleolar organizing regions) of acrocentric chromosomes number 13, 14, 15, 21 and 22. Moreover, tau-1 immunostaining shows that this protein is colocalized with the protein nucleolin interacting with pre-rRNA transcripts as well as

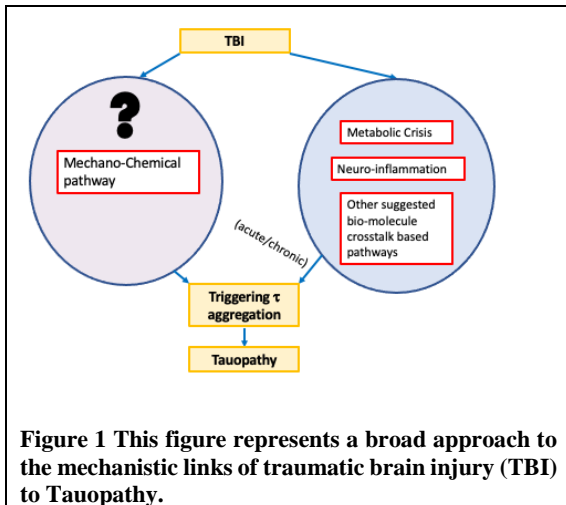
some ribosomal proteins in the dense fibrillar parts of the nucleolus; therefore it has been concluded that tau putatively has a role in ribosomal formation, chromatin structure and nucleocytoplasmic transport. Recent research has shown that the expression of APP (amyloid precursor protein) in chromosome 21 is correlated with tau and nucleolin structure and disruption of the physiological state, for instance aggregation, could lead to deleterious production of APP resulting in its miscleavage and amyloid beta formation (Sjöberg *et al.*, 2006).

In dendrites, tau is responsible for dendritic spine development, elongation and maturation. All tau isoforms contribute to this role to a certain extent. Based on studies in rodents' young neurons for analysis of dendritic spine formation, 0N3R tau participates in the structure of elongated spine necks while 2N4R forms the spine heads. Other isoforms such as 1N4R has an intermediate effect on spine maturation, length and number (placing it between 0N4R and 2N4R), while 1N3R tau increases these parameters (Zempel *et al.*, 2017).

MECHANISTIC LINKAGE OF TRAUMATIC BRAIN INJURY TO TAU PROTEIN

AGGREGATION

In the upcoming sections, the previously studied proposed mechanisms linking traumatic brain injury to tau protein aggregation as well as the pathway explored in the experimental section of this thesis are explored.



THE METABOLIC CRISIS CASCADE

Traumatic brain injury (TBI) induces rapid movement of the brain and this mechanical deformation causes indiscriminate release of neurotransmitters from neurons. These neurotransmitters, including glutamate, open postsynaptic channels resulting in ionic disruptions. The changes in glutamate and K^+ efflux are short-lived (1-5minutes) after injury, the time course is dependent on injury severity. In experimental models of moderate TBI in the adult rat, this increase in extracellular fluid K^+ concentration does not exceed the physiological ceiling and can be resolved by the uptake mechanisms of glial cells (Kawamata *et al.*, 1992). This increase short-lived commencing instantly after injury being resolved within less than 10 minutes (Giza and Hovda, 2014).

In addition to K^+ changes, glutamate binding to the postsynaptic NMDA receptors leads to calcium (Ca^{2+}) influx. In contrast to the short-lived K^+ efflux, the time course of calcium influx are age-dependent. In all age groups (Post-natal day 17, 28 and adult) the immediate increase in Ca^{2+} is resolved between 2-4 days post injury in most structures. However, in

PND28 and adult rats there was a delayed secondary thalamic increase in Ca^{2+} influx between day 2-14 post injury. Given the mitochondrial role in calcium uptake and high levels of intracellular calcium after injury, excess intra mitochondrial calcium accompanied by low ATP/ADP ratio as observed after impact leads to mitochondrial swelling via the Mitochondrial Permeability Transition pathway (Duchen, 1999) that could contribute to the non-apoptotic decrease of mitochondrial population (Prins *et al.*, 2013), causing further energy depletion and possibly the repetition and ongoing of this cycle. In addition, Ca^{2+} activates free radical generating enzymes such as NADPH oxidase, xanthine oxidase, lipases and phospholipases, alongside the generic decrease of performance of cellular scavenging systems and mitochondrial electron transfer chain impairment oxidative stress is elevated in the cell. Using different markers of oxidative stress lead to inconsistent results; but overall, experiments suggest that the onset of free radical formation and reaching to a significant level above baseline starts within few hours after injury and is resolved between 12-24 hours after (Prins *et al.*, 2013).

This release of excitatory amino acids (EAAs) and ionic fluxes increase the cerebral need for energy as neurons struggle to re-establish ionic equilibrium. The Na^+/K^+ -ATPase consumes ATP as it pumps ions back across the membranes, which increases consumption of glucose to replenish ATP stores. The time course of glucose uptake after TBI has been well characterized across different injury severities and age groups. Immediately after injury there is an increase in cerebral metabolic rates of glucose (CMRg) which lasts for 6hrs post injury. This phase of hyperglycolysis is thought to be in response to increase Na^+/K^+ -ATPase activity. Following this phase, the brain enters a state of CMRg depression

that can last for days-weeks in animal models depending on injury severity and age. Glucose metabolic depression can persist for weeks to months in human TBI. During these changes in glucose metabolism there are also changes in cerebral blood flow (CBF). Decreases in cerebral blood flow (with no evident change in systemic plasma glucose levels) (Giza and Hovda, 2014) has been reported during the acute increased energy needs, leading to an early “uncoupling” event. Both CBF and CMRg remain depressed for days to weeks depending on the age and injury severity and motor, cognitive and behavioral deficits have been observed during this time.

After TBI, based on experiments in rat models there is primarily a global decrease of cerebral blood flow, later on sparing the hindbrain and therefore becoming limited to the region of damage; this transition was observed within 15 minutes, 1 hours and 2 hours respectively (Yamakami and McIntosh, 1989).

The magnitude of the post TBI metabolic crisis is injury severity dependent. Increasing injury severities can activate additional mechanisms (Kawamata *et al.*, 1992). The post injury K^+ increase is considerably higher than the physiological ceiling levels, which surpasses the capacity of glial cell uptake resulting in larger and longer lasting increases in K^+ compared to mild TBI (Katayama *et al.*, 1990). In addition, the rise of extracellular K^+ leads to the depolarization of neuronal terminals and Ca^{2+} mediated exocytosis of glutamate that causes another wave of depolarization (Katayama *et al.*, 1990). In contrast to mild injury, the pattern of this release is focal in the beginning of the injury and expands with time. Decrease of CBF that approach near-ischemic levels can result in exacerbation of glutamate release (Vespa *et al.*, 1998). The levels of intracellular calcium caused by

intense glutamate release lead to calcium mediated mitochondrial dysfunction, increasing oxidative stress inside the cell. Reactive oxidative species (ROS) bind to DNA causing damage and activating poly(ADP-ribose) polymerase (PARP); after 8 hours from severe controlled cortical impact injury in mice, elevation in PARP-1 (a subtype of PARP) was reported, persisting for a period of 24 days. Elevation of PARP depletes the cell of NAD⁺ and contributes to aggravating the metabolic crisis, causing cell death in extreme conditions (Prins *et al.*, 2013).

Transient increase of intracellular calcium (2-5 min) leads to prolonged increase of Tau phosphorylation (1-4h) depending on the lasting of high intracellular concentrations of calcium. This phosphorylation is done by GSK2beta enzyme at the Tau-1 epitope on a Tyrosine residue; that could be inhibited by lithium administration and genistein, a noncompetitive Tyrosine kinase inhibitor(Hartigan and Johnson, 1999) (Mattson, Engle and Rychlik, 1991). Also, it has been suggested that calcium related tau phosphorylation can occur via calcium calmodulin dependent kinase activation. Increased oxidative stress alike the state of increased free radicals post-TBI; was shown to significantly have positive effects on Tau phosphorylation on Ser-396, Thr 205, Ser 404, Ser 214 epitopes (Melov *et al.*, 2007).

THE NEUROINFLAMMATION CASCADE

Neuroinflammation is not a simple concept as there are positive and negative consequences to activation of differential pathways. Even though inflammation and activation of immune cells is necessary for clearing cellular debris and damage and their absence will be detrimental, the disproportional upregulation of pro-inflammatory systems can be

problematic, both acutely and chronically. In this section, the role of resident and circulating immune cells that have entered the brain as a result of BBB (blood brain barrier) disruption, the signaling factors and their effect on inducing tau phosphorylation will be reviewed. For evaluating the temporal profile of resident glial cell activation and also presence of activated circulatory immune cells in the brain, various experimental methods of TBI have been used including FP (fluid percussion) injury, CCI (cortical contusion injury) and weight-drop injury. In the experimental trauma model literature, time periods less than 24h after injury are considered the acute phase, between 24-168h subacute and from 1 week onwards chronic. In this section, some examples using experimental models of this sort is discussed.

Reactive Glia Function Cascades. In the absence of any triggering factors, microglia are in a resting state known as M0. Following brain injury, cytokines are released and the presence of cellular debris triggers activation of the residing macrophages. The activated microglia are classified in a spectrum between M1-like and M2-like phenotype, which have different inflammation profiles and characteristics. M2-like's activation is considered anti-inflammatory or neuroprotective, being triggered by IL-4 and IL-13 and secreting anti-inflammatory cytokines such as IL-10 and TGF β and other factors including arginase and mannose receptors. In contrast, M1-like microglial phenotype is considered pro-inflammatory with more phagocytic activity. M1-like phenotype is activated by INF gamma and excess of extracellular K⁺ concentrations, secretes IL-1beta, IL-4, IL-6, IL-23 and TNFalpha; restricting repair of tissue and having more inflammatory action; it is the

neurodegenerative phenotype and contributes to damage. While M1 microglia secrete inflammatory cytokines and reactive oxygen species, that further contribute to the blood brain barrier disruption and aggravation of inflammation, the M2-like phenotype secrete regulatory and wound healing factors: TGF- β , IL-10 and Arginase 1, Chitinase and extracellular matrix components respectively(Wang *et al.*, 2013).

Following TBI, the M2-like phenotype activation is known to be a short-lived response and after a week M1 is the dominating microglia phenotype in the area of the lesion(Wang *et al.*, 2013) A study conducted on rats that were exposed to mild CCI (cortical contusion injury) and euthanized between 1 to 14 days showed an increase in the markers of M2 activation after 1-3 days, peaking at 3-5 days and decreasing after 7 days towards baseline by 14 days(Myer *et al.*, 2006).

In addition, correlation has been shown between the injury severity and M1-like type microglia activation, but not for M2-like type (Perry, Nicoll and Holmes, 2010). Mild FP injury, injecting saline with a force of 1.5 atm resulted in axonal damage and accumulation of APP (amyloid precursor protein) and neuronal loss specially in the corpus callosum (most vulnerable to injury due to force dynamics) and persistent microglial activation and inflammation for at least 2 weeks(Cortez, McIntosh and Noble, 1989).Shortly after TBI, the excitotoxicity and potassium efflux (discussed in the previous section) leads to severity dependent microglial activation. Induction of epileptiform excitotoxic activity in rat hippocampus using kainic acid lead to the observation of increased microglial activation depicted by histological changes in correlation with the increase of kainic acid concentration in the environment and the time of exposure to the given condition before

being washed out. There is a correlation between injury severity and magnitude and duration of excitatory activity and K⁺ ion concentration increase. The mechanism of activation of pro-inflammatory microglia as a result of excitotoxicity is putatively mediated by the microglial ionotropic receptors that upon activation by kainate and other glutamate agonists lead to significantly increased TNF alpha secretion 2 hours after administration in cultured rat microglia via binding to the GluR2 subunit(Ábrahám *et al.*, 2001).

Reactive astrocytes. Similar to microglia, reactive astrocytes have variant profiles based on mechanism of activation. The A1 phenotype is activated by inflammatory cytokines, such as INF gamma, TNF alpha, IL-1beta that are secreted by M1 reactive microglia and A2 phenotype is activated by ischemia(Wang *et al.*, 2013). The outcome of A1 activation, based on studies is known to be neurodegenerative, and A2 astrocytes contribute to repair and neuro-regeneration after ischemic brain injury. IFN gamma induces the differentiation of astrocytes to the A2 phenotype (Choi,2005) via the Jak1/stat3 pathway. The secretome of A2 is considered “M2-like”; including Chitinase like 3 (Chil 3), Arginase, Frizzled Receptor (Fzd)(Liddelow and Barres, 2017).

Astrocytes respond and produce many classes of molecules. Another class of chemicals generally released by reactive astrocytes are damage associated molecular patterns (DAMPs) such as high mobility group box-1, heat shock proteins and S-100 group of proteins(Burda, Bernstein and Sofroniew, 2016). DAMPs are known to bind to pattern recognition receptors such as toll like receptors (TLRs) and RAGE (receptors for advanced glycation end products) on microglia, circulating phagocytic immune cells and also astrocytes themselves; the autocrine effect on astrocytes leads to the secretion of TNF

alpha. S100beta protein induces the formation of calcium channels in phosphatidyl serine membrane leading to influx of calcium in nervous tissue cells(Karve, Taylor and Crack, 2016). As previously mentioned, trauma-activated astrocytes with the A1 phenotype contribute to neuroinflammation; they secrete IL-1-beta (that in an autocrine manner further increases IL-1b), IL-6, IL-8 and INF alpha and MMP9 (matrix metalloproteinase)(Liddelow and Barres, 2017)

Temporal Profile of Acute Post TBI Cytokine Secretion After TBI, a gamut of cytokines are released from various classes of cells including glia, endothelia and neurons therefore increase of a certain factor can seldom be attributed to a single type of cell. In this section, models in which solely evaluate the temporal profile of cytokines are analyzed. Experimental research on this parameter has commonly been done in human models with severe traumatic brain injury; in these studies, patients were evaluated for a period of less than seven days and there was no follow-up in the sub-acute phase. Another limitation to these studies that does not allow drawing firm conclusions is the heterogeneity of the values estimated for the time of cytokine peaking in the CSF in comparison to serum levels. However, experimental traumatic brain injury with a broader time span has been done on rats. A microdialysis study in patient revealed an increase of IL-1beta, TNF-alpha and IL-6 few hours up to a day after injury; however, these cytokines decreased in the following days and reached serum levels in the end of the analysis period. Specifically, cytokines such as IL-6 and IL-8 and S100B protein rise 6 hours post injury and decrease gradually thereafter; while IL-beta, IL-alpha, TNF-alpha stay considerably above serum levels (2-100 fold) in the first 24 hours after trauma(Morganti-Kossmann *et al.*, 1997). Another

microdialysis study on patients with severe diffuse traumatic brain injury shows that inflammatory cytokines including IL-1beta, TNF-alpha, IL-6 and IL-8 peaks vary in a range of 1 to 3 days post-trauma(Helmy *et al.*, 2011). Another study comparing between jugular venous and arterial concentrations of cytokines detected considerably higher concentrations of IL-6 in jugular venous blood particularly after 48 hours post trauma(Mckeating *et al.*, 1997). In non-human primates, the secretion of inflammatory cytokines (such as IL-1, TNF-alpha and IL-6) is repressed months after injury but still is prominent, measured 1,6 and 12 months after injury. Studies in rat have predominantly been done on early post traumatic concentrations of inflammatory cytokines. In both models of cortical contusion and fluid percussion injury there was an increase of IL-1beta and TNF-alpha expression in mononuclear cells and astrocytes within 6 hours or less after injury(Fan *et al.*, 1996) A study done by Holmin *et al.* showed that there is a delayed increase of IL-beta and TNF-alpha expression 4-6 days in the local and distal areas of the brain in a control cortical contusion model of traumatic brain injury(Holmin *et al.*, 1997). In a moderate weight-drop TBI model, rats were followed for 3 months and after euthanization TNF- alpha and IL-1beta positive cells were seen in the ipsilateral cortex of the lesion; this immunoreactivity was slightly less than of 2 weeks post injury(Holmin and Mathiesen, 1999).

Blood-Brain Barrier Disruption. In a physiologic state, the blood brain barrier's tight junction will not allow inflammatory cytokines or immune cells from the peripheral circulation to enter the brain. However, following traumatic brain injury disruption of the

BBB allows peripheral immune agents can be infiltrated to the brain. The mechanical motion of the brain during TBI can disrupt the microvasculature and also the endogenous factors released in the brain following injury, lead to increase permeability of this tight barrier. Initially, the BBB breakdown in addition to the initial impact is due to several components, including post-traumatic excitotoxicity and imbalance of Na⁺, K⁺ and Ca²⁺, secretion of matrix metalloproteinase and inflammatory cytokines such as IL-1beta; as IL-1beta by binding to its receptors on endothelial cells of the BBB assists its breakdown.(Pylayeva-Gupta, 2011).

Stretching of blood vessels leads to the influx of plasma albumin into the brain resulting in the increase of [Ca²⁺] in microglia, inducing activation, IL-1 synthesis and NO production(Hooper, Taylor and Pocock, 2005). These activated cells also release TNF-alpha, that have multiple autocrine and paracrine effects, such as leading to decreased occludin expression and astrocytic and endothelial chemokine secretion. In addition, TGF-beta released by brain parenchymal cells as an aftermath of injury leads to decreased Claudin and VE-Cadherin expression; these phenomena integratively resulting in the weakening of BBB. Of other factors produced by multiple cell types following TBI, MMP (Matrix Metalloproteinase) 2,3 and 9 can be named that disrupt basal lamina and junction proteins(Alves, 2014) one of the cell types that releases this enzyme are astrocytes (Pylayeva-Gupta, 2011). Following injury, neurons have been detected to release chemokines such as MIP-1/CXCL2, CCL2/MCP-1, IL-8/CXCL8, CCL20, CCL21. MIP-2/CXCL2, MCP-1/CCL2, IL-8/CXCL8 are known to be responsible for leucocyte infiltration, which is further assisted by the weak BBB. Release of these chemokines is an

acute and intrinsic response of neurons; for instance, 4h after injury MCP-1/CCL2 is solely detected in neurons and peaks after 8-12h.

Focal injuries in contrast to diffuse injuries result in leucocyte invasion to a higher extent. Focal injuries are characterized by the lining of dura and sub-dura matter being invaded by neutrophilia; these cells invade the parenchyma after 2 days. Lining of the vasculature by monocytes happens by 12h after injury, after 3-6 days and accommodation of these cells to the injured tissue monocytes become the predominant cell type present in the lesion. This invasion by peripheral immune cells exacerbates the inflammation and degeneration. Worsening damage to the brain microvasculature as described above leads to microbleeds and accumulation of iron and oxidative stress. The disruption of the brain microvasculature occurs in a wide range of injury severities, a study of American football college athletes who had been exposed to sub-concussive and concussive hits during a football game had increased levels of blood S100 β and S100 β auto-antibody; the levels of S100 β auto antibodies correlate to the impulse control and postural stability test outcomes analyzed post-season.

A study designed for analysis of microvasculature pathology of moderate CCI (2.5 mm of compression distance) assessed the effect of trauma on progress of pathology in acute, subacute and chronic periods; microbleeds were first observed at the sites of injury after 24 hours and proceeded to increase until 3 months after injury. In addition, IgG staining showed increase of this protein at early time points around contusion foci, remaining higher than normal until up to 3 months. Increased microglial and astrocytic activation were also seen in the mentioned time period; microglia morphing into a bush-like shape in the chronic

phase and astrocytes being localized around microbleeds(Igarashi, Potts and Noble-Haeusslein, 2007). BBB disruption has also been proven to be a lingering outcome of TBI; lasting for years in patients with mild TBI (according to their measured GCS, >13) and having considerable correlation with the occurrence of post traumatic epilepsy, which exacerbates the condition itself (Tomkins *et al.*, 2008).

A study conducted by Johnson et al. on a human cohort with long term TBI survival (ranging between 1-47 years, mean of 17 years) showed that the white matter generation and microgliosis are evident up to 18 years after single TBI. In the same study, granular axonal bulbs (suggestive of axonal terminal disconnection) staining positive for APP were seen in brains of individuals with long term survival of TBI; in those on the higher end of long term survival demyelination was prominent. In addition, one of the features observed in the mentioned cohort was axonal loss; most perceptible in the corpus callosum. In the study done on rhesus monkeys, the most visible axonal loss was in the thalami(Johnson *et al.*, 2013). Regarding the persistence of inflammation after single mild TBI there is a considerable amount of discrepancy in literature; some such as the study mentioned above argue that a single mild TBI could cause neuroinflammation that persists for years; on the other hand, some argue that a single mild TBI sets off a transient neuro-inflammation as a study on adult mice suggests. This study exposed a group of adult mice to single mild TBI and another to 42 mild injuries throughout 7 days. The group exposed to single injury did not show considerable microglial activation, and the astrocyte activation and phosphorylated tau presence were not seen after one month (except a minute focal

reactivation of astrocytes after 6 months) whilst in the group sustaining multiple injuries showed persistent microgliosis and tau hyperphosphorylation and biphasic astrocyte activation resolving at 1 month and reappearing at 6 months.

Effect of Immune Phenomena on Amyloid beta formation and Tau Phosphorylation. The direct and indirect effects of pro-inflammatory cytokines on protein aggregate formation has been well studied. However, information regarding roles of anti-inflammatory cytokines and other factors released by the injured tissue and its' surrounding penumbra on tau post translational modifications are yet to be elaborated upon.

Following TBI, clinically relevant pathophysiological levels of tumor necrosis factor- α (TNF), interleukin-6 (IL-6) and interleukin-1 β (IL-1 β) are shown to be present as explained in the previous sections. These cytokines effect the formation of deleterious protein aggregates(Buxbaum *et al.*, 1992). A number of pro-inflammatory cytokines are known to induce tau protein hyperphosphorylation. The binding of immune cell derived IL-beta and IL-6 to their receptors on the surface of neurons activated tau kinases; IL-beta induces MAPK-p38 activation, not only by binding to IL-R but also by inducing iNOS (inducible nitric oxide synthase). IL-6 induces tau phosphorylation via the cdk5/p35 pathway(Mrak and Griffin, 2005), and it has been proposed that IL-6 secreted by astrocytes leads to calcium influx through NMDA receptors therefore activating the mentioned kinase. In addition to these cytokines, S100B protein released in response to brain trauma upregulates IL-6 secretion, APP production and calcium influx(Li *et al.*, 2011). It should be noted that CCR2 monocyte-mediated neutrophil infiltration to the brain correlates with tau protein

phosphorylation and inhibition of this process decreases lesion size and phosphorylated tau immunoreactivity(Gyoneva *et al.*, 2015).

A NEW ANGLE TO LOOK AT THE RELATION OF TRAUMATIC BRAIN INJURY TO TAU PROTEIN AGGREGATION

All the previous pathways mentioned have a criterion in common; they all involve biochemical alteration to tau protein (phosphorylation has been the one usually studied). However, we hypothesized that in absence of biochemical alteration, CNS tau protein can aggregate as a direct result of mechanical force; testing and confirmation of this hypothesis is elaborated on in the upcoming chapters.

CHAPTER 2: INTRODUCTION TO FLOW-INDUCED CRYSTALLIZATION

In the field of polymer physics, it has long been known that applied mechanical strains (shear or extensional strains) cause flows that promote the assembly of polymers into semi-crystalline states via flow-induced crystallization (FIC). The application of strains to flowing polymer systems increases the number of nucleation sites and accelerates the kinetics of crystallization. Flows of sufficient strength, orientation and velocity gradients stretch and align polymer chains lowering the entropy of the uncrystallized, assembling system and, as a consequence, reduce the change in the free energy required for molecular associations to occur (Mackley and Keller, 1975). The effect of flows in assembling systems can have profound effects on the rate of formation of crystalline structures, lowering the time to crystallization from hours to hundredths of a second in some polymer systems (an acceleration of over 5 orders of magnitude) (Hass and Maxwell, 1969). This effect has been utilized throughout industry to produce profound directional strength changes in many materials that we take for granted (e.g. film-blown polyester bottles with biaxial crystal orientation in the plane of the bottle wall enabled the storage of carbonated drinks) (Rao and Rajagopal, 2001). However, the effect of flows caused by applied mechanical stress on the assembly biomolecular systems has received very little attention. In 2015, (Young *et al.*, 2015) examined the accelerated crystallization of streptavidin in a planar film, concluding that shear effects were responsible for the enhanced crystallization rate by increasing the rate of nucleation (Young *et al.*, 2015). In 2016, (Paten *et al.*, 2016) demonstrated that collagen

fibrils (a semi-crystalline oriented structure) could be “flow-crystallized” by application of an extensional strain to droplets comprising monomeric precursor molecules.

FLOW-INDUCED AGGREGATION

Flow-induced aggregation on the other hand differs from flow-induced crystallization in that the final structures produced are not crystalline in nature, but are polymorphic aggregations of the precursor molecules which comprise them. Following up on anecdotal reports that stirring or agitation of solutions accelerated the rate of amyloid fibril formation (Hill *et al.*, 2006). demonstrated systematically that shear flow induces fibril aggregation in solutions of β -lactoglobulin(Hill *et al.*, 2006). In a follow up, (Dunstan *et al.*, 2009) showed that shear flow promoted amyloid-Beta fibrilization, possibly via alignment of aggregates followed by adhesion. However, shear flows have limited orientational capabilities relative to extensional flows, which necessarily stretch fluids and the molecules with them. In 2017, (Dobson *et al.*, 2017) devised a low volume system which permitted the assessment of the relative importance of shear and extensional flows to the flow-induced aggregation of proteins. They conclude the extensional flows can induce protein unfolding, exposing binding sites and that the effectiveness of the flow on aggregation is dependent on the topology, structure, concentration and sequence of the protein (Dobson *et al.*, 2017). Importantly, Dobson et al. found that extensional strains can induce protein aggregation during millisecond exposures and at relatively low concentrations (as low as 0.5 mg/ml).

RHEOLOGY OF SMALL SAMPLES

Rheology provides information on the visco-elastic properties of complex fluids, which are directly related to the molecular structure of the fluid. One of the biggest challenges in performing rheology on biological samples is availability of sample material. Shear rheometers and extensional rheometers generally require liquid sample sizes larger than 100 μl . Shear rheology, in particular, is extremely challenging for samples with volumes below 10 μl , as special care is required to make accurate measurements (Clasen, Gearing and McKinley, 2006). However, biological samples are often limited in volume because their isolation is difficult or their production is prohibitively expensive (Sharma *et al.*, 2018). Recently, a simple extensional rheology system was developed that can be used to characterize the extensional properties of samples of complex fluid with volumes down to $\sim 10 \mu\text{l}$ (Dinic, Biagioli and Sharma, 2017). Given that that our protein of interest (τ) costs \$10,000 per ml, a system that can accurately extract the complex rheological behavior from samples with volumes below 10 μl would be quite valuable.

TAU IN TRAUMATIC BRAIN INJURY AND LOCALIZATION OF TAU AGGREGATION TO REGIONS OF HIGH STRAIN

Tau is a structural protein synthesized in neurons and contributes to axonal stability through interaction with microtubules (Wang and Mandelkow, 2016). Tau can also be secreted from neurons and enter into the extracellular space, where it may enter the CSF or eventually, the blood. Aggregates of phosphorylated tau have been implicated in

neurodegenerative disorders, including Alzheimer Disease, Fronto-Temporal Dementia and, more recently CTE(Zetterberg *et al.*, 2006). Deposition of phospho-tau described in CTE neuropathological specimens has shown a propensity to occur in the depths of cerebral sulci and in perivascular areas, which has implicated biomechanical strain (and strain-rates) as a potential factor for tau aggregation following repetitive mild traumatic brain injury or concussion(Ghajari, Hellyer and Sharp, 2017). CTE is associated with head trauma from activities that produce focused mechanical effects in perivascular areas within the cerebral sulci. Computational modelling predicts that impacts during sporting events such as American football can produce strains up to 40% and, more critically, strain rates that approach 150 Hz(Ghajari, Hellyer and Sharp, 2017) in these same locations. Given this data and recent investigations that have demonstrated that extensional strains can directly cause aggregation of proteins, we hypothesized that mechanical deformations (strains and strain rates) cause tau protein to aggregate via flow-induced aggregation effects. To test our hypothesis, we developed a microrheological method capable of applying extensional strains to microvolumes of tau protein solutions.

CHAPTER 3: MATERIALS AND METHODS

Materials

The tau protein isoform chosen for our experiments was 3R0N with a molecular weight of 36.7kDa purchased from Boston Biochem (#SP-497, Cambridge, MA, USA). A three repeat tau isoform was chosen due to its higher efficiency in aggregation as 4R repeat tau protein due to having two cysteine residues is prone to forming intramolecular cysteine disulfide. Also, addition of N-terminals would delay fibrillization, therefore an isoform with no N-Terminal insertions was used.

As we intended to assess the effect of extensional strain on tau protein solution, the concentration used had to be in a range in which tau fibrillization was expected, independent of the introduction of additional chemicals to the solution. Previous experiments have shown that tau will fibrillize spontaneously between 200 μ M – 400 μ M. It is noteworthy that in the experiments used to define this range, the protein solution required incubation times in excess of 2-4 weeks (Kuret *et al.*, 2005). In our experiment the tau was subjected to rapid strain to induce aggregation. For these experiments, we have also set the tau concentration below overlap concentration. The overlap concentration C^* from dilute to semi-dilute regimes is defined as the concentration at which the polymer coils touch one another. Tau protein is classified as a random coil polymer. Thus, the corresponding formula was used to determine its theoretical overlap concentration(Ying and Chu, 1987):

$$C^* = \frac{M}{N_A \left(\frac{h_0}{2}\right)^3} \quad (1)$$

Where M is the molecular weight of the protein, N_A Avogadro's number and h_0 the root mean square of the end to end distance of the polymer. The end-to-end distance in good solution was measured via the hard-sphere method by Jho et al. (Jho *et al.*, 2010) and for the smallest non-phosphorylated tau isoform was 16.6nm. Per these calculations $\overline{C^*} = 106.5 \text{ mg/ml}$ or 2.9 mM. We will maintain our solution well below this value at (10 mg/ml), ensure that it is in the dilute regime will thus be unbiased by polymer interactions intrinsic to the solution. Tau was solvated in PBS solution at a pH of 7.4 and an ionic strength of 162.7 mM.

To benchmark our rheometer we selected a molecule, PEO (poly-ethylene oxide), with nearly the same molecular weight as tau (35kDa; PEO35) and with the same concentration as our tau solution (10mg/ml). While PEO is not a direct molecular equivalent to tau (wormlike chain vs. flexible), it has well-known rheological properties and is available in varying molecular weights. To observe the effect of molecular weight on the readout of our micro-rheometer, PEO (@100kDa; PEO100) was also examined at the same concentration. For both PEO molecules, which we assumed to be worm-like chains, their estimated overlap concentration was determined using:

$$C^* = \frac{\phi}{N_A} \frac{2^3}{[\eta]} \quad (2)$$

were $\phi = 1.7 \times 10^{21}$ is the Flory constant, $[\eta] = 4.33 \times 10^{-4} M_w^{0.67}$ dl/g is the intrinsic viscosity. The calculated values of overlap concentrations are $C_{35kDa}^* = 48.72$ mg/ml, and $C_{100kDa}^* = 24.23$ mg/ml.

Since both overlap concentrations were at least double our working concentration of 10 mg/ml, we felt comfortable proceeding with the PEO35 and PEO100 to benchmark our rheometer and to provide some insight on the effect of molecular weight on the readout. The PEO was solvated in distilled water.

METHODS

Tau Shear Rheology

Because there is no available viscosity data on tau in shear, some of the tau solution was tested in a standard cone and plate stress-controlled shear rheometer. The solution was kept at -70°C until test day when it was thawed in an ice water bath at 5°C until use.

Experiments were all done at 25°C and ambient humidity (60% at the time of testing).

An AR-2000 (TA instruments, New Castle, De, USA) with a 20 mm diameter cone and plate geometry was used to measure the rheological properties of the tau protein solution.

We have used two procedures for this experiment: creep and peak hold with a 1 μ Nm torque applied on the sample over 6 minutes. Due to the delicate structure of the solution and its low viscosity we kept the torque at a minimum. The resultant displacement was recorded that can be used to calculate the rheological properties of Tau protein. In the creep test creep compliance intercept (J_0) and viscosity ($\sqrt{\mu}$) of the fluid are reported.

Creep compliance intercept provides information on the elasticity of the polymer. To be

consistent with the extensional rheology tests, sample temperature for both experiments was set at 25 °C. However, the low viscosity of the solution limited the shear rates that could be tested to ~30 Hz. Due to limited sample volume, multiple experiments could not be run.

MICROEXTENSIONAL RHEOLOGY

Because extensional rheology has a more profound effect on the aggregation of proteins (Dobson *et al.*, 2017), we developed a simple microrheometer capable of applying

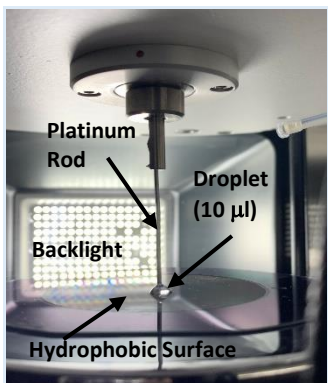


Figure 2. Microrheological test apparatus. A droplet of tau solution was placed on a hydrophobic surface and extensionally strained using a platinum rod.

a large range of strain rates on a very small volume sample.

The tau solution was kept at -70°C until test day when it was thawed in an ice water bath at 5°C until use. Experiments were all done at room temperature (22°C) and ambient humidity (60% at the time of testing). Figure 2 shows the general test set

up. The instrument used to test the tau protein droplets was a tensiometer (K-100, KRUSS GMBH) with a platinum rod probe operated in the Contact Angle setting. Tau containing

droplets were placed on a hydrophobic surface, through modified surface roughness on silicon wafer, to provide sufficient depth for insertion of the tensiometer probe. Detachment of the probe from liquid surface was filmed at 36k frames per second by a high speed camera (Phantom V7, Vision Research). Movies were analyzed in MATLAB software based a program provided to us courtesy of Prof. Vivek Sharma as shown in (Dinic *et al.*, 2014) From the liquid bridge thinning data which are measured as the normalized droplet radius thinning as a function of time, there are two regions of interest:

1) The approach to the visco-elastic regime and 2) the visco-elastic regime itself. In the visco-elastic regime, the relaxation time can be extracted with the corresponding model(Del Giudice, Haward and Shen, 2017):

$$\frac{R(t)}{R_0} = \left(\frac{G_E R_0}{2\sigma} \right)^{1/3} \exp\left(\frac{-t}{3\lambda_E} \right) \quad (3)$$

Where $R(t)$ is the instantaneous radius of the liquid bridge, R_0 is the initial radius of the liquid bridge, G_E is elastic modulus, σ is surface tension, t is time, and λ_E is extensional relaxation time. Prior to the formation of of a liquid thread, the response to strain is an inertia-capillary response to which the corresponding equation is fit(Pooler, Usardi and Hanger, 2010):

$$\frac{R(t)}{R_0} = 0.8 \left(\frac{\sigma}{\rho R_0} \right)^{1/3} \left(\frac{t_c - t}{R_0} \right)^{2/3} \quad (4)$$

where σ is the solution surface tension, ρ is density, t_c is the breakup time.

For the experiments on the tau protein droplets a total of 48 tests were run (16 droplets with 3 repeats). For the *comparative controls*, PEO35 and PEO100 were run under similar conditions to the tau and for each, a minimum of three repeats were performed, the results are shown in the following figures.

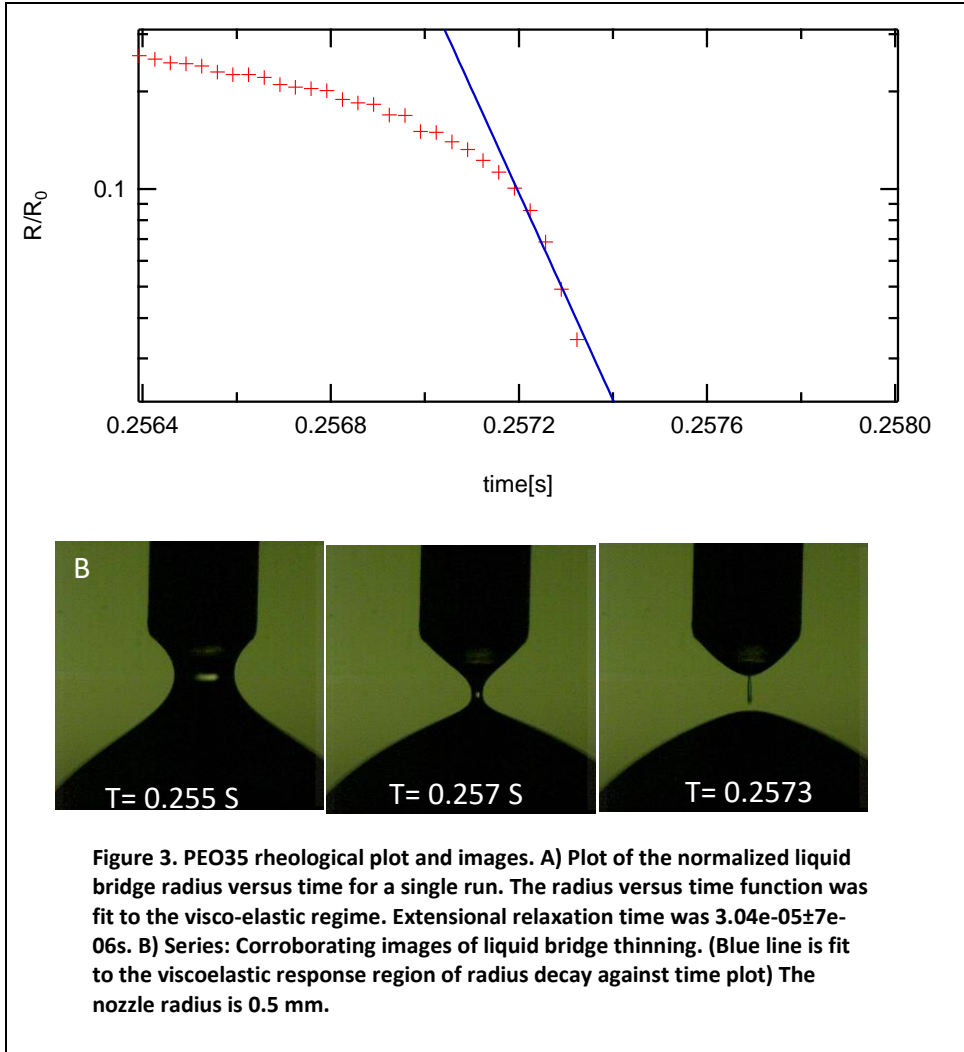


Figure 3. PEO35 rheological plot and images. A) Plot of the normalized liquid bridge radius versus time for a single run. The radius versus time function was fit to the visco-elastic regime. Extensional relaxation time was $3.04e-05 \pm 7e-06$ s. B) Series: Corroborating images of liquid bridge thinning. (Blue line is fit to the viscoelastic response region of radius decay against time plot) The nozzle radius is 0.5 mm.

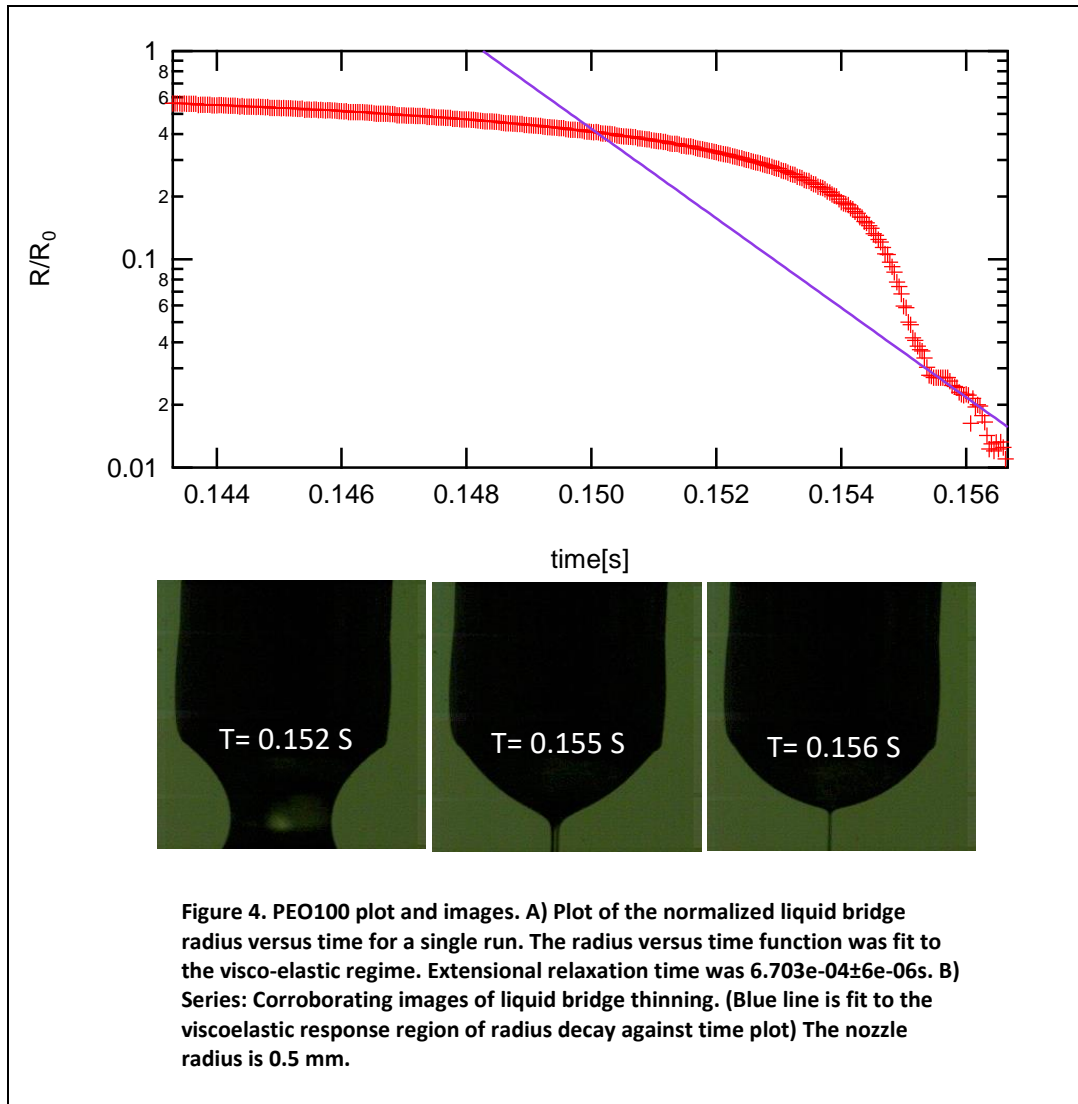


Figure 4. PEO100 plot and images. A) Plot of the normalized liquid bridge radius versus time for a single run. The radius versus time function was fit to the visco-elastic regime. Extensional relaxation time was $6.703e-04 \pm 6e-06$ s. B) Series: Corroborating images of liquid bridge thinning. (Blue line is fit to the viscoelastic response region of radius decay against time plot) The nozzle radius is 0.5 mm.

CHAPTER 4: RESULTS

TAU SHEAR RHEOLOGY

The tau protein shows a very weak elastic behavior of $E = 3.77 \times 10^{-3} \pm 2 \times 10^{-4}$ Pa and viscosity of $\eta = 1.59 \times 10^{-2} \pm 2 \times 10^{-3}$ Pa s, which are 15 times higher than water. We did not observe any variation of viscosity as a function of shear rate up to 30 Hz. As these values are very close to the lower limit of the available commercial rheometers, and the fluid can be considered approximately Newtonian.

PEO MICRORHEOLOGY BENCHMARKING

Supplementary Figures 1 and 2 describe the two benchmarking solutions of small and large molecular weight: PEO35 and PEO100. Briefly, as expected, PEO35 and PEO100 exhibited clear differences in behavior with the larger molecule producing durable thread and a longer lasting visco-elastic regime. In addition, the experiments showed average extensional relaxation times which were lower for the smaller PEO35 (3.04×10^{-5} s) than they were for the PEO100 (6.703×10^{-4} s). The microrheological assay also detected clear elastic behavior in the PEO100 at higher extensional strain rates. The comparative controls demonstrated that our approach produces expected results for the two molecules that were tested. The strain rate at which the smaller molecule entered the visco-elastic regime was 10 kHz.

TAU MICROEXTENSIONAL RHEOLOGY

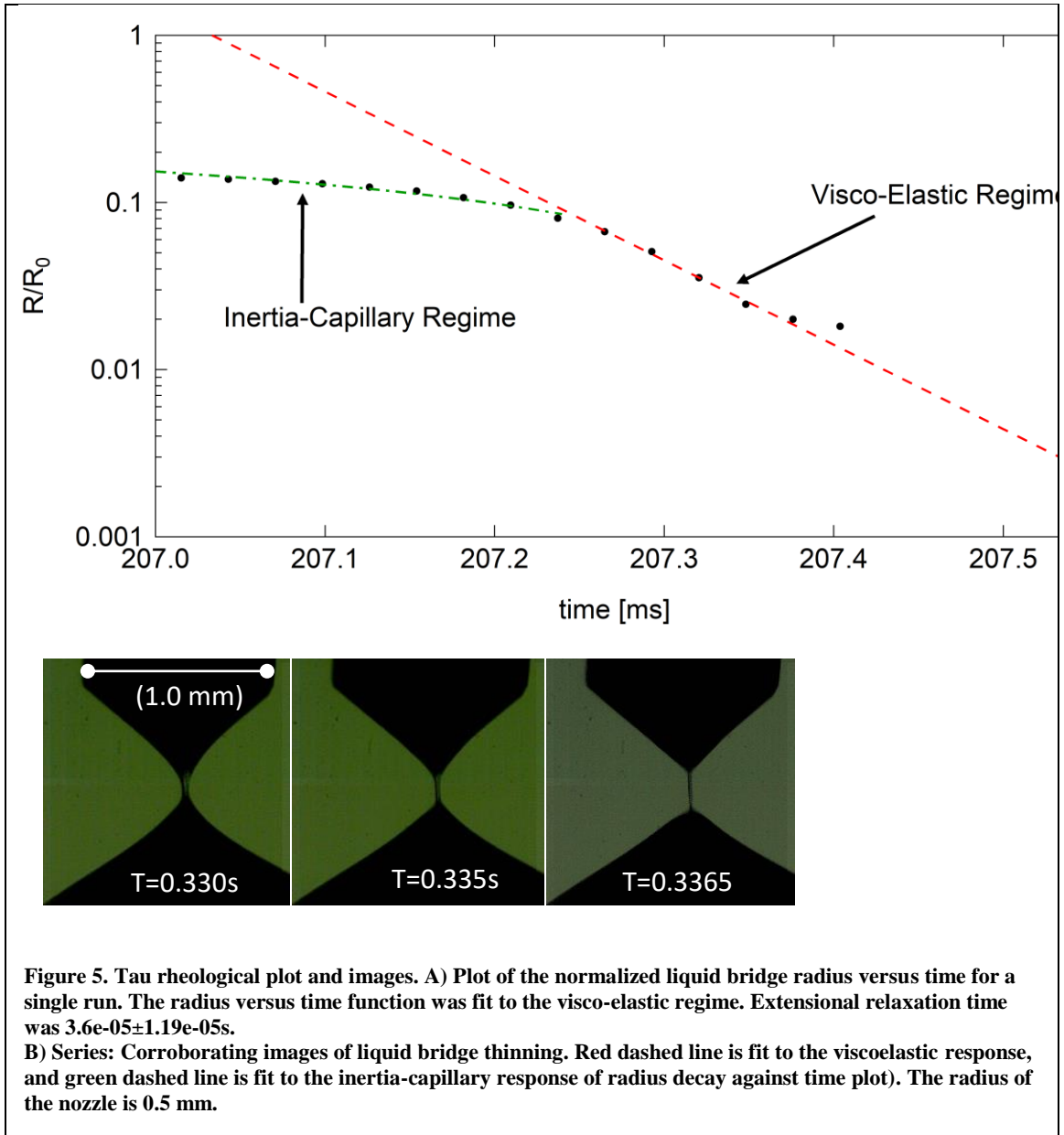


Figure 5 shows a representative liquid bridge radius vs. time curve and photos of an actual experiment for the tau solution. The extensional relaxation time for the tau was 3.6×10^{-5} s which is very close to the relaxation time found for the PEG35 solution.

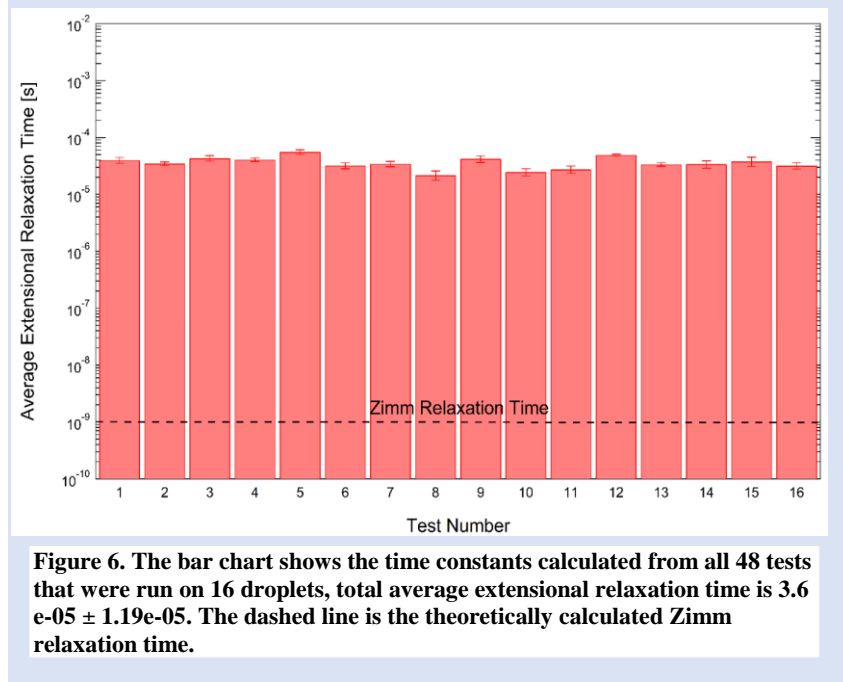


Figure 6 is a compilation of all 48 tests showing the consistency of the experiment and the measured time constant relative to the theoretical or Zimm time constant.

ANALYSIS

For every polymer, there is a theoretical extensional relaxation time that can be calculated using the Zimm theory (Del Giudice, Haward and Shen, 2017):

$$\lambda = F \frac{[\eta]M_w\eta_s}{RT} \quad (5)$$

In the case of Tau protein, $[\eta]$ is equal to this random coil's intrinsic viscosity, the corresponding equation is (Ying and Chu, 1987):

$$[\eta] = \frac{\phi(h_0)^3}{M_w} \quad (6)$$

Where ϕ (Flory's Constant) is 1.7×10^{21} , h_0 is the end to end distance that for Tau 3R 0N = 16.6 nm, M_w (molecular weight)=36.7 kDa, η_s (solvent's viscosity- water at 25°C) = 8.9×10^{-4} , Pa s, F is a parameter dependent on the solvent quality (through the dimensionless scaling exponent $\nu=0.3$) giving: $F \cong 0.55$. R (universal gas constant) = 8.314 J / (mol. · K), Absolute temperature = 295° K. Solving gives us a final value for Zimm relaxation time of 1.6 ns.

The average extensional relaxation time obtained from our experiments was $\cong 36.0 \mu\text{s}$; 5 orders of magnitude higher than the theoretical prediction. The onset of the visco-elastic regime was at a Wi of 0.4 suggesting that aggregation of tau began at an extensional strain rate of $\sim 11\text{k Hz}$.

The relationship between Zimm time constant and the molecular weight is known to have the form of (Larson, 1999).

$$\lambda_{zimm} \sim (M_w)^{1.8} \quad (7)$$

As the formula above depicts, Zimm relaxation time highly dependent on the molecular weight of particles in the polymer solution. Therefore, this increase of Zimm relaxation time could be attributed to formation of particles with higher molecular weight suggesting flow-induced aggregation.

CHAPTER 5: DISCUSSION

We have conducted a fairly circumscribed investigation into the hypothesis that tau protein (specifically the 3R0N isoform) undergoes flow-induced aggregation when subjected to mechanical extensional strains. Because of the expense of tau (and many other biological molecules) we developed a very low volume microrheological method based on the work of Vivek Sharma's lab (Dinic *et al.*, 2017), (Dinic *et al.*, 2017) to test the hypothesis. The system permitted us to perform 48 individual extensional tests on 16 separate microdroplets of the tau solution. The results, which were robust and consistent, suggested that tau monomers in solution will aggregate when subjected to a single extensional strain. While this result supports our hypothesis, the strain rates required to induce molecular aggregation were far higher than strain rates estimated to occur during head trauma experienced in sports such as American football¹⁸. Thus, it would seem that direct mechanochemical effects may not cause tau aggregation under physiological conditions. However, there are four very important considerations. The first thing to consider is the relaxation time of tau, which we estimated to be about 1.5 ns based on a Zimm calculation. The relaxation time of tau will depend very strongly on the local concentration and molecular crowding which can vary substantially depending on where the tau is located in the cell (e.g. on the microtubules) or in the extracellular fluid. Relaxation times can lengthen considerably under crowded conditions. Recently, it was shown that collagen (which has a relaxation time of 1/7000 sec in dilute solution) can be flow-crystallized at 0.5 Hz when crowded to 5 times its overlap concentration (Paten *et al.*, 2016). The second consideration is the state of phosphorylation of the tau protein. It

has been shown that tau fibrils often include large amount of hyperphosphorylated tau(Del Giudice, Haward and Shen, 2017), which we did not examine here.

Hyperphosphorylated tau may aggregate more readily and have a longer relaxation time and lower overlap concentration. Third, extensional strain rates, which are the most important driver of flow-induced aggregation, depend on the initial separation distance of objects that are being extended. If there are stiff materials that are being separated rapidly (e.g. microtubules fracturing), the extensional strains created between the separating ends can be quite high. Theoretically, at $t=0^+$ the velocity gradient is singular during the initial separation. Finally, the cellular environment is complex in terms of containing metal ions, increased oxidative stress especially at times of injury that increase the propensity of tau protein to aggregate(Pooler, Usardi and Hanger, 2010), presence of polyanions such as nucleic acids; that facilitate tau polymerization. Physiological ionic strength is also different from the solution used in experiments, being approximately 120 mM (Larson, 1999), that due to being lower, is relatively facilitative to tau protein fibrillization(Schliwa, 2002). As we now know tau to be capable of flow-induced aggregation experimentally, it is possible that flow-induced tau aggregation may occur under physiological conditions during impact events. This represents a novel plausible mechanism of protein accumulation with the potential to lead to significant biological consequences.

CHAPTER 6: CONCLUSIONS AND FUTURE WORK

While our methods have aimed to emulate the impact of head injury on neurons and therefore on tau protein, the strain rates caused by head trauma in a contact sport such as American football have been reported much lower than our experimental conditions (Ghajari, Hellyer and Sharp, 2017), initially suggesting that the effect demonstrated in our experiments. However, aside from the complexity of the cellular environment and the existence of chaperone proteins such as Hsp90 that regulate tau protein aggregation (Blair *et al.*, 2013), the breakage of microtubules also contributes to release tau protein to the cytoplasm and increase of local concentrations; it is noteworthy that concentration has a direct association with Zimm relaxation time.

To build up on the results obtained in this study, an additional experiment could be injection of the post-strain tau protein solution to animal model brains and perform behavioral studies and post-mortem histopathology and compare results with traumatic brain injury animal models.

In addition, as chronic traumatic encephalopathy has yet to be recognized as a separate disease (McKee *et al.*, 2013); the pathology of patient brains' with history of multiple brain trauma has been consistent with the pathology observed in Motor Neuron Disease, Lewy body dementia and Pick's disease analysis of the impact of mechanical force on the protein markers of the aforementioned such as alpha synuclein and TAR-DNA binding protein can be valuable to establish whether neurotrauma increases the propensity of individuals to

develop previously discovered neurodegenerative disease or does it in reality lead to a completely new pathology.

REFERENCES

- Ábrahám, H. *et al.* (2001) 'Rapid activation of microglial cells by hypoxia, kainic acid, and potassium ions in slice preparations of the rat hippocampus', *Brain Research*, 906(1–2), pp. 115–126. doi: 10.1016/S0006-8993(01)02569-0.
- Alves, J. L. (2014) 'Blood-brain barrier and traumatic brain injury', *Journal of Neuroscience Research*, 92(2), pp. 141–147. doi: 10.1002/jnr.23300.
- Avila, J. *et al.* (2004) 'Role of Tau Protein in Both Physiological and Pathological Conditions', *Physiological Reviews*, 84(2), pp. 361–384. doi: 10.1152/physrev.00024.2003.
- Biology, M. S.-N. R. M. C. and 2002, undefined (no date) 'The evolving complexity of cytoplasmic structure', *nature.com*. Available at: https://idp.nature.com/authorize/casa?redirect_uri=https://www.nature.com/articles/nrm781&casa_token=IXLyIXZPamUAAAAA:NrFRKJkvEiaHnfjooubCIavl-25BSIIsoRM4q8IIUm8H50evi-kmQD9E_2si0_D3Bb85hMXqcicAADvqLdk.
- Blair, L. J. *et al.* (2013) 'Accelerated neurodegeneration through chaperone-mediated oligomerization of tau', *Journal of Clinical Investigation*, 123(10), pp. 4158–4169. doi: 10.1172/JCI69003.
- Buée, L. *et al.* (2000) 'Tau protein isoforms, phosphorylation and role in neurodegenerative disorders', *Brain Research Reviews*, 33(1), pp. 95–130. doi:

10.1016/S0165-0173(00)00019-9.

Burda, J. E., Bernstein, A. M. and Sofroniew, M. V. (2016) ‘Astrocyte roles in traumatic brain injury’, *Experimental Neurology*. Elsevier Inc., 275, pp. 305–315. doi:

10.1016/j.expneurol.2015.03.020.

Buxbaum, J. D. *et al.* (1992) ‘Cholinergic agonists and interleukin 1 regulate processing and secretion of the Alzheimer β /A4 amyloid protein precursor’, *Proceedings of the National Academy of Sciences of the United States of America*, 89(21), pp. 10075–10078.

doi: 10.1073/pnas.89.21.10075.

Chirita, C. N., Necula, M. and Kuret, J. (2003) ‘Anionic micelles and vesicles induce tau fibrillization in vitro’, *Journal of Biological Chemistry*, 278(28), pp. 25644–25650. doi:

10.1074/jbc.M301663200.

Clasen, C., Gearing, B. P. and McKinley, G. H. (2006) ‘The flexure-based microgap rheometer (FMR)’, *Journal of Rheology*, 20.

Cortez, S. C., McIntosh, T. K. and Noble, L. J. (1989) ‘Experimental fluid percussion brain injury: vascular disruption and neuronal and glial alterations’, *Brain Research*, 482(2), pp. 271–282. doi: 10.1016/0006-8993(89)91190-6.

Dinic, J. *et al.* (no date) ‘Pinch-off dynamics and dripping-onto-substrate (DoS)

rheometry of complex fluids’, *pubs.rsc.org*. Available at:

<https://pubs.rsc.org/en/content/articlehtml/2017/lc/c6lc01155a>.

Dinic, J., Biagioli, M. and Sharma, V. (2017) ‘Pinch-off dynamics and extensional relaxation times of intrinsically semi-dilute polymer solutions characterized by dripping-onto-substrate rheometry’, *Journal of Polymer Science, Part B: Polymer Physics*. John

- Wiley and Sons Inc., 55(22), pp. 1692–1704. doi: 10.1002/POLB.24388.
- Dobson, J. *et al.* (2017) ‘Inducing protein aggregation by extensional flow’, *Proceedings of the National Academy of Sciences*. Proceedings of the National Academy of Sciences, 114(18), pp. 4673–4678. doi: 10.1073/pnas.1702724114.
- Duchen, M. R. (1999) ‘Contributions of mitochondria to animal physiology: From homeostatic sensor to calcium signalling and cell death’, *Journal of Physiology*, 516(1), pp. 1–17. doi: 10.1111/j.1469-7793.1999.001aa.x.
- Dunstan, D. E. *et al.* (2009) ‘Shear flow promotes amyloid- fibrilization’, *Protein Engineering Design and Selection*. Oxford University Press (OUP), 22(12), pp. 741–746. doi: 10.1093/protein/gzp059.
- Fan, L. *et al.* (1996) ‘Experimental brain injury induces differential expression of tumor necrosis factor- α mRNA in the CNS’, *Molecular Brain Research*, 36(2), pp. 287–291. doi: 10.1016/0169-328X(95)00274-V.
- Ghajari, M., Hellyer, P. J. and Sharp, D. J. (2017) ‘Computational modelling of traumatic brain injury predicts the location of chronic traumatic encephalopathy pathology’, *Brain*, 140(2), pp. 333–343. doi: 10.1093/brain/aww317.
- Del Giudice, F., Haward, S. J. and Shen, A. Q. (2017) ‘Relaxation time of dilute polymer solutions: A microfluidic approach’, *Journal of Rheology*. Society of Rheology, 61(2), pp. 327–337. doi: 10.1122/1.4975933.
- Giza, C. C. and Hovda, D. A. (2014) ‘The new neurometabolic cascade of concussion’, *Neurosurgery*, 75(3), pp. S24–S33. doi: 10.1227/NEU.0000000000000505.
- Goedert, M. and Jakes, R. (1990) ‘Expression of separate isoforms of human tau protein:

correlation with the tau pattern in brain and effects on tubulin polymerization.’, *The EMBO Journal*, 9(13), pp. 4225–4230. doi: 10.1002/j.1460-2075.1990.tb07870.x.

Gyoneva, S. *et al.* (2015) ‘Ccr2 deletion dissociates cavity size and tau pathology after mild traumatic brain injury’, *Journal of Neuroinflammation*. *Journal of Neuroinflammation*, 12(1), pp. 1–12. doi: 10.1186/s12974-015-0443-0.

Hartigan, J. A. and Johnson, G. V. W. (1999) ‘Transient increases in intracellular calcium result in prolonged site- selective increases in Tau phosphorylation through a glycogen synthase kinase 3 β -dependent pathway’, *Journal of Biological Chemistry*, 274(30), pp. 21395–21401. doi: 10.1074/jbc.274.30.21395.

Hass, T. W. and Maxwell, B. (1969) ‘Effects of shear stress on the crystallization of linear polyethylene and polybutene-1’, *Polymer Engineering and Science*, 9.

Helmy, A. *et al.* (2011) ‘The cytokine response to human traumatic brain injury: Temporal profiles and evidence for cerebral parenchymal production’, *Journal of Cerebral Blood Flow and Metabolism*, 31(2), pp. 658–670. doi: 10.1038/jcbfm.2010.142.

Hill, E. K. *et al.* (2006) ‘Shear Flow Induces Amyloid Fibril Formation’, *Biomacromolecules*. American Chemical Society (ACS), 7(1), pp. 10–13. doi: 10.1021/bm0505078.

Holmin, S. *et al.* (1997) ‘Delayed cytokine expression in rat brain following experimental contusion’, *Journal of Neurosurgery*, 86(3), pp. 493–504. doi: 10.3171/jns.1997.86.3.0493.

Holmin, S. and Mathiesen, T. (1999) ‘Long-term intracerebral inflammatory response after experimental focal brain injury in rat’, *NeuroReport*, 10(9), pp. 1889–1891. doi:

10.1097/00001756-199906230-00017.

Hooper, C., Taylor, D. L. and Pocock, J. M. (2005) 'Pure albumin is a potent trigger of calcium signalling and proliferation in microglia but not macrophages or astrocytes', *Journal of Neurochemistry*, 92(6), pp. 1363–1376. doi: 10.1111/j.1471-4159.2005.02982.x.

Igarashi, T., Potts, M. B. and Noble-Haeusslein, L. J. (2007) 'Injury severity determines Purkinje cell loss and microglial activation in the cerebellum after cortical contusion injury', *Experimental Neurology*, 203(1), pp. 258–268. doi: 10.1016/j.expneurol.2006.08.030.

Jho, Y. *et al.* 2010 'Monte carlo simulations of tau proteins: effect of phosphorylation', *Elsevier*. Available at: <https://www.sciencedirect.com/science/article/pii/S0006349510008003>.

Johnson, V. E. *et al.* (2013) 'Inflammation and white matter degeneration persist for years after a single traumatic brain injury', *Brain*, 136(1), pp. 28–42. doi: 10.1093/brain/aws322.

Karve, I. P., Taylor, J. M. and Crack, P. J. (2016) 'The contribution of astrocytes and microglia to traumatic brain injury', *British Journal of Pharmacology*, 173(4), pp. 692–702. doi: 10.1111/bph.13125.

Katayama, Y. *et al.* (1990) 'Massive increases in extracellular potassium and the indiscriminate release of glutamate following concussive brain injury', *Journal of Neurosurgery*, 73(6), pp. 889–900. doi: 10.3171/jns.1990.73.6.0889.

Kawamata, T. *et al.* (1992) 'Administration of excitatory amino acid antagonists via

microdialysis attenuates the increase in glucose utilization seen following concussive brain injury', *Journal of Cerebral Blood Flow and Metabolism*, 12(1), pp. 12–24. doi: 10.1038/jcbfm.1992.3.

Khatoon, S., Grundke-Iqbal, I. and Iqbal, K. (1992) 'Brain Levels of Microtubule-Associated Protein τ Are Elevated in Alzheimer's Disease: A Radioimmuno-Slot-Blot Assay for Nanograms of the Protein', *Journal of Neurochemistry*, 59(2), pp. 750–753. doi: 10.1111/j.1471-4159.1992.tb09432.x.

Kuret, J. *et al.* (2005a) 'Pathways of tau fibrillization', *Biochimica et Biophysica Acta - Molecular Basis of Disease*, 1739(2), pp. 167–178. doi: 10.1016/j.bbadis.2004.06.016.

Kuret, J. *et al.* (2005b) 'Pathways of tau fibrillization', *Biochimica et Biophysica Acta (BBA) - Molecular Basis of Disease*. Elsevier, 1739(2–3), pp. 167–178. doi:

10.1016/J.BBADIS.2004.06.016.

Li, C. *et al.* (2011) 'Astrocytes: Implications for Neuroinflammatory Pathogenesis of Alzheimers Disease', *Current Alzheimer Research*, 8(1), pp. 67–80. doi:

10.2174/156720511794604543.

Liddel, S. A. and Barres, B. A. (2017) 'Reactive Astrocytes: Production, Function, and Therapeutic Potential', *Immunity*. Elsevier Inc., 46(6), pp. 957–967. doi:

10.1016/j.immuni.2017.06.006.

Mackley, M. R. and Keller, A. (1975) 'Flow Induced Polymer-Chain Extension and Its Relation to Fibrous Crystallization', *Phil Trans Roy Soc Lon*, 278(1276), pp. 29-.

Mattson, M. P., Engle, M. G. and Rychlik, B. (1991) 'Effects of elevated intracellular calcium levels on the cytoskeleton and tau in cultured human cortical neurons',

- Molecular and Chemical Neuropathology*, 15(2), pp. 117–142. doi: 10.1007/BF03159951.
- McKeating, E. G. *et al.* (1997) ‘Transcranial cytokine gradients in patients requiring intensive care after acute brain injury’, *British Journal of Anaesthesia*, 78(5), pp. 520–523. doi: 10.1093/bja/78.5.520.
- McKee, A. C. *et al.* (2013) ‘The spectrum of disease in chronic traumatic encephalopathy’, *Brain*, 136(1), pp. 43–64. doi: 10.1093/brain/aws307.
- Melov, S. *et al.* (2007) ‘Mitochondrial oxidative stress causes hyperphosphorylation of tau’, *PLoS ONE*, 2(6). doi: 10.1371/journal.pone.0000536.
- Morganti-Kossmann, M. C. *et al.* (1997) ‘Production of cytokines following brain injury: Beneficial and deleterious for the damaged tissue’, *Molecular Psychiatry*, 2(2), pp. 133–136. doi: 10.1038/sj.mp.4000227.
- Mrak, R. E. and Griffin, W. S. T. (2005) ‘Glia and their cytokines in progression of neurodegeneration’, *Neurobiology of Aging*, 26(3), pp. 349–354. doi: 10.1016/j.neurobiolaging.2004.05.010.
- Myer, D. J. *et al.* (2006) ‘Essential protective roles of reactive astrocytes in traumatic brain injury’, *Brain*, 129(10), pp. 2761–2772. doi: 10.1093/brain/awl165.
- Papasozomenos, S. C. (1997) ‘The heat shock-induced hyperphosphorylation of τ is estrogen- independent and prevented by androgens: Implications for Alzheimer disease’, *Proceedings of the National Academy of Sciences of the United States of America*, 94(13), pp. 6612–6617. doi: 10.1073/pnas.94.13.6612.
- Paten, J. A. *et al.* (2016) ‘Flow-Induced Crystallization of Collagen: A Potentially

Critical Mechanism in Early Tissue Formation', *ACS Nano*. 2016/04/14, 10(5), pp. 5027–5040. doi: 10.1021/acsnano.5b07756.

Perry, V. H., Nicoll, J. A. R. and Holmes, C. (2010) 'Microglia in neurodegenerative disease', *Nature Reviews Neurology*. Nature Publishing Group, 6(4), pp. 193–201. doi: 10.1038/nrneurol.2010.17.

Pooler, A. M., Usardi, A. and Hanger, D. P. (2010) 'Dynamic association of tau with neuronal membranes is regulated by phosphorylation and the tyrosine kinase fyn', *Alzheimer's & Dementia*. The Alzheimer's Association, 6(4), pp. S277–S278. doi: 10.1016/j.jalz.2010.05.916.

Prins, M. *et al.* (2013) 'The pathophysiology of traumatic brain injury at a glance', *DMM Disease Models and Mechanisms*, 6(6), pp. 1307–1315. doi: 10.1242/dmm.011585.

Pylayeva-Gupta, Y. (2011) '基因的改变 NIH Public Access', *Bone*, 23(1), pp. 1–7. doi: 10.1038/jid.2014.371.

Rao, I. J. and Rajagopal, K. R. (2001) 'A study of strain-induced crystallization of polymers', *Int J Solids Struct*, 38(6), pp. 1149–1167.

Reynolds, M. R. *et al.* (2006) 'Peroxy-nitrite-mediated τ modifications stabilize preformed filaments and destabilize microtubules through distinct mechanisms', *Biochemistry*, 45(13), pp. 4314–4326. doi: 10.1021/bi052142h.

Schweers, O. *et al.* (1994) 'Structural studies of tau protein and Alzheimer paired helical filaments show no evidence for β -structure', *Journal of Biological Chemistry*, 269(39), pp. 24290–24297.

Sharma, A. M. *et al.* (2018) 'Tau monomer encodes strains', *eLife*. eLife Sciences

Publications Ltd, 7. doi: 10.7554/eLife.37813.

Sjöberg, M. K. *et al.* (2006) ‘Tau protein binds to pericentromeric DNA: A putative role for nuclear tau in nucleolar organization’, *Journal of Cell Science*, 119(10), pp. 2025–2034. doi: 10.1242/jcs.02907.

Tapia-Rojas, C. *et al.* (2019) ‘It’s all about tau’, *Progress in Neurobiology*, 175(December 2018), pp. 54–76. doi: 10.1016/j.pneurobio.2018.12.005.

Timm, T. *et al.* (2008) ‘Structure and regulation of MARK, a kinase involved in abnormal phosphorylation of Tau protein’, *BMC Neuroscience*, 9(SUPPL. 2), pp. 1–6. doi: 10.1186/1471-2202-9-S2-S9.

Tomkins, O. *et al.* (2008) ‘Blood-brain barrier disruption in post-traumatic epilepsy’, *Journal of Neurology, Neurosurgery and Psychiatry*, 79(7), pp. 774–777. doi: 10.1136/jnnp.2007.126425.

Vespa, P. *et al.* (1998) ‘Increase in extracellular glutamate caused by reduced cerebral perfusion pressure and seizures after human traumatic brain injury: A microdialysis study’, *Journal of Neurosurgery*, 89(6), pp. 971–982. doi: 10.3171/jns.1998.89.6.0971.

Wang, G. *et al.* (2013) ‘Microglia/macrophage polarization dynamics in white matter after traumatic brain injury’, *Journal of Cerebral Blood Flow and Metabolism*, 33(12), pp. 1864–1874. doi: 10.1038/jcbfm.2013.146.

Wang, Y. and Mandelkow, E. (2016) ‘Tau in physiology and pathology’, *Nature Reviews Neuroscience*. Nature Publishing Group, pp. 5–21. doi: 10.1038/nrn.2015.1.

Yamakami, I. and McIntosh, T. K. (1989) ‘Effects of traumatic brain injury on regional cerebral blood flow in rats as measured with radiolabeled microspheres’, *Journal of*

Cerebral Blood Flow and Metabolism, 9(1), pp. 117–124. doi: 10.1038/jcbfm.1989.16.

Ying, Q. and Chu, B. (1987) ‘Overlap Concentration of Macromolecules in Solution’, *Macromolecules*, 20(2), pp. 362–366. doi: 10.1021/MA00168A023.

Young, J. E. *et al.* (2015) ‘Flow-induced 2D protein crystallization: characterization of the coupled interfacial and bulk flows’, *Soft Matter*. Royal Society of Chemistry (RSC), 11(18), pp. 3618–3628. doi: 10.1039/c5sm00429b.

Zempel, H. *et al.* (2017) ‘Axodendritic sorting and pathological missorting of Tau are isoform-specific and determined by axon initial segment architecture’, *Journal of Biological Chemistry*, 292(29), pp. 12192–12207. doi: 10.1074/jbc.M117.784702.

Zetterberg, H. *et al.* (2006) ‘Neurochemical aftermath of amateur boxing’, *Archives of Neurology*. American Medical Association, 63(9), pp. 1277–1280. doi:

10.1001/archneur.63.9.1277.